

A novel method for a nanosized ZSM-5 (MFI) zeolite synthesis in proton form

Alexey G. Dedov,^{a,b} Alexander A. Karavaev,^{*a,b} Alexey S. Loktev,^{a,b} Malikha N. Vagapova,^a Kirill A. Cherednichenko,^b Konstantin I. Maslakov,^c Alexey A. Sadovnikov^a and Sergey P. Molchanov^a

^a A. V. Topchiev Institute of Petrochemical Synthesis, Russian Academy of Sciences, 119991 Moscow, Russian Federation. E-mail: aleksankaray@yandex.ru

^b National University of Oil and Gas 'Gubkin University', 119991 Moscow, Russian Federation

^c Department of Chemistry, M. V. Lomonosov Moscow State University, 119991 Moscow, Russian Federation

DOI: 10.1016/j.mencom.2024.04.039

A new method for the synthesis of nanosized ZSM-5 zeolite with the MFI structure in the proton form is reported. The material was synthesized by the hydrothermal-microwave method and characterized by X-ray diffraction, scanning electron microscopy, transmission electron microscopy, atomic force microscopy, low-temperature nitrogen physisorption, thermal desorption of ammonia and solid-state ^{27}Al NMR. The synthesized material is formed by zeolite particles of 30–80 nm in size, which ensures its high specific surface area, pore volume and interparticle porosity.

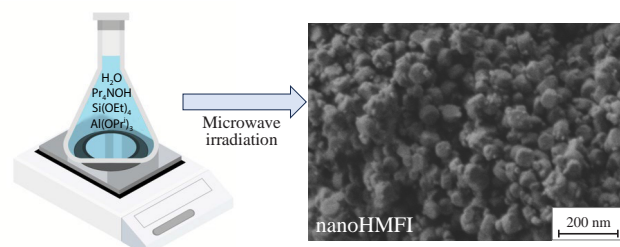
Keywords: nanosized ZSM-5 zeolite, MFI, hydrothermal-microwave synthesis, proton form, micro/mesopores, interparticle porosity.

ZSM-5 zeolites (structural type MFI – mordenite framework inverted) are widely used as effective catalysts in several processes of oil refining and petrochemistry.^{1–8} These materials are characterized by the availability of Brønsted and Lewis acid centers, high specific surface area, thermal stability and the presence of a microporous structure that provides a molecular sieve effect.

A significant amount of the acid centers in ZSM-5 zeolites is located in channels of about 0.5 nm in size.⁹ Such small channel size hinders the diffusion of many reagents to acid centers localized in these channels. In addition, ZSM-5 zeolite-based catalysts are deactivated during carbonation of microporous channel inlets. One approach to reduce diffusion limitations and problems associated with carburization is to use the nanosized zeolite catalysts.^{10–19}

Nanosized zeolites (<100 nm in size) demonstrate high specific surface area with the significant contribution from the external surface and the interparticle porosity. Due to the smaller particle size, nanosized zeolites contain higher amount of inlet openings of zeolite channels per unit of external surface, and they also have smaller micropore length. As a result, diffusion restrictions are reduced, which facilitates the access of raw material molecules to the active centers localized in the channels. The combination of these properties can contribute to slowing down deactivation of catalysts and increasing their stability.^{20–24}

Most of the reported methods for the synthesis of nanosized zeolites require the preparation of several initial solutions,^{23,24} long-term 'aging' of the initial mixtures of reagents and, in some cases, the preliminary synthesis of seed crystals.²⁵ Also, these synthesis techniques typically produce nanosized zeolites in the sodium form, and an additional stage of the multiple ion exchange is required to convert them into the proton form.^{24,26}



The hydrothermal-microwave method allows intensifying and simplifying the synthesis of ZSM-5 zeolites. The microwave treatment evenly and quickly heats the reaction mixture, which significantly reduces the crystallization time of the zeolite.²⁷ However, there is little literature data on the microwave radiation synthesis of nanosized zeolite ZSM-5 in the proton form. Earlier,²⁸ nanosized zeolite ZSM-5 in proton form was obtained by the preliminary mixing of the initial gel ('aging' of the initial mixture) for 48 h, followed by crystallization in two stages: 90 min at 80 °C and 30 min at 120 °C. The synthesized ZSM-5 zeolite²⁸ mainly contained particles of 80 nm in size. Even a slight raising the duration of the second stage of crystallization and temperature caused an increase of the zeolite particle size.²⁸

The aim of our work has been to develop a new technique of the nanosized ZSM-5 zeolite hydrothermal-microwave synthesis directly in the proton form, thus significantly reducing the average size of the zeolite particles.[†] As a result, in a number of petrochemical processes, this reduction may contribute to the increased stability of the catalysts based on the nanoH-ZSM-5.

[†] To synthesize nanosized zeolite directly in the proton form,²⁹ a mixture containing Si(OEt)₄ (99%, Sigma-Aldrich), distilled water, Pr₄NOH (1 M, Alfa Aesar) and Al(OPr)₃ (>98%, Sigma-Aldrich) was prepared. Molar ratio of reagents was Si(OEt)₄ : H₂O : Pr₄NOH : Al(OPr)₃ = 1 : 4.33 : 0.25 : 0.00608.

Tetra-*n*-propylammonium hydroxide and tetraethylorthosilicate were dissolved in distilled water and intensively stirred at 75 °C for 6 h. Then aluminum isopropoxide was added to the resulting gel and the mixture was stirred until complete homogenization, but without subsequent aging. The resulting suspension was placed in a Teflon autoclave and subjected to microwave treatment in the Berghof SpeedWave 4 system (maximum power 1500 W, 2.45 GHz). Crystallization was carried out at 214 °C for 3.5 h. The obtained particles of nanosized zeolite, designated

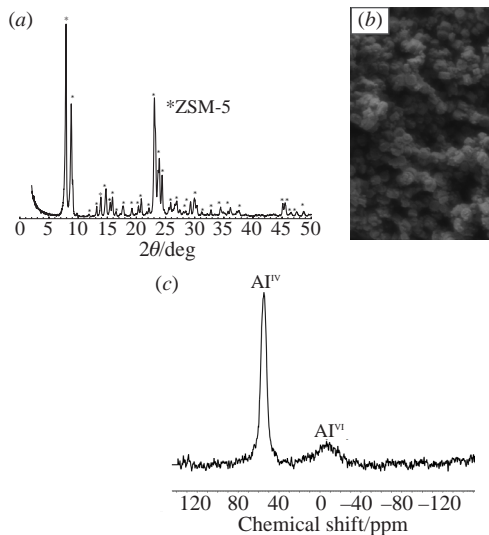


Figure 1 Characterization of synthesized nanoH-ZSM-5 zeolite: (a) XRD pattern, (b) SEM-microimage and (c) ^{27}Al MAS NMR spectrum.

The XRD pattern of the synthesized nanosized zeolite powder is shown in Figure 1(a). The characteristic peaks in the 2θ ranges of 8–9° and 23–25° confirm the crystallite structure of the synthesized ZSM-5 zeolite according to the ICDD database. The relative degree of crystallinity determined from the relative intensities of the peaks at 23–25° was 86%. According to the X-ray fluorescence analysis, the silica modulus (molar ratio $\text{SiO}_2/\text{Al}_2\text{O}_3$) of the synthesized zeolite was 196.

Scanning electron microscopy (SEM) of the obtained zeolite revealed nanosized particles with the shape typical for ZSM-5 zeolites and the developed interparticle porosity [Figure 1(b)].

The ^{27}Al MAS NMR spectrum [Figure 1(c)] contains the peak with the chemical shift of 54–55 ppm, which corresponds to tetrahedrally coordinated aluminum ions (Al^{IV}) incorporated in the zeolite framework. There is also a low-intense peak with the chemical shift of 0 ppm related to octahedrally coordinated (out-of-frame) aluminum ions (Al^{VI}). These data show that almost all aluminum ions are incorporated in the zeolite structure.

The formation of nanosized zeolite ZSM-5 particles was confirmed by the transmission electron microscopy data (TEM) [Figure 2(a)]. The particle size distribution in the powder of synthesized zeolite was estimated from the TEM data [Figure 2(b)]. Particles ranging in size from 30 to 80 nm are dominating in the synthesized material. The average particle size in the obtained zeolite is much smaller than those in the nanosized ZSM-5 zeolite synthesized *via* microwave irradiation.²⁸ The interplanar distance in crystallites of the obtained material determined by TEM [Figure 2(c)] was 1.2 nm, which agrees with the reference data for {101} plane of calcined ZSM-5 reported on the website of the International Zeolite Association.

The atomic force microscopy (AFM) image of the synthesized zeolite powder [Figure 3(a)] agrees with the SEM data. At larger magnifications, the aggregated nature of large ZSM-5 zeolite particles becomes visible. The AFM probe registered presence of the small particles in the aggregate at a distance of 20–30 nm from each other. The interplanar distance in a small zeolite particle determined by TEM, along with the comparison of the AFM image in Figure 3(a) with the TEM data [Figure 3(b)], allow us to suggest that particles of the synthesized nanosized ZSM-5 zeolite are aggregates of the smaller particles of 20–30 nm in size.

as nanoH-ZSM-5, were isolated by centrifugation in an ultracentrifuge at a rotation speed of 2000 rpm followed by washing with distilled water, drying at 190 °C for 2 h and calcination in air at 550 °C for 7 h to remove the organic template.

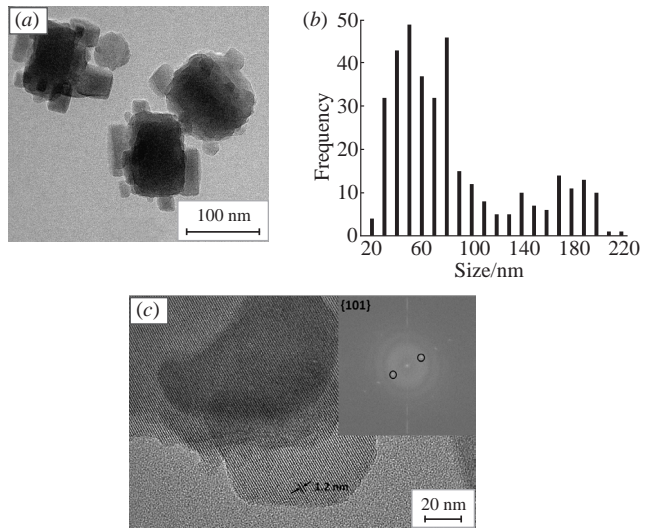


Figure 2 TEM data for synthesized nanoH-ZSM-5 zeolite: (a) images of aggregates, (b) particle size distribution, (c) high resolution image of a small particle (interplanar distance is shown).

In Table 1 the textural parameters of the obtained nanoH-ZSM-5 zeolite are compared with those of H-ZSM-5 zeolite with the particle size over 1 μm synthesized *via* the hydrothermal microwave method.³⁰ NanoH-ZSM-5 zeolite demonstrates higher specific surface area and total pore volume, as well as a micro-mesoporous structure due to the presence of nanosized particles and interparticle porosity. It is noteworthy that the external specific surface area, total pore volume and mesopore volume of nanoH-ZSM-5 significantly exceed the values for H-ZSM-5 zeolite with particle sizes over 1 μm.

The total number of acid centers in the nanoH-ZSM-5 in the proton form measured by the temperature programmed desorption of ammonia was 195 $\mu\text{mol g}^{-1}$. The distribution of acid centers by their strength is shown in Figure 4. NanoH-ZSM-5 shows a bimodal distribution, with ammonia desorption maxima at 178 °C and 386 °C. The numbers of weak and strong acid centers in the nanoH-ZSM-5 zeolite are 105 and 90 $\mu\text{mol g}^{-1}$, respectively.

In Table 2 the acidic properties of the synthesized nanoH-ZSM-5 zeolite are compared with those of H-ZSM-5 zeolite with the particle sizes larger than 1 μm synthesized by the hydrothermal microwave method.³⁰ The values of the total

Table 1 Textural parameters of nanoH-ZSM-5 and H-ZSM-5 zeolites.

Sample	$S_{\text{BET}}/ \text{m}^2 \text{g}^{-1}$	$S_{\text{ext}}^a/ \text{m}^2 \text{g}^{-1}$	$S_{\text{micro}}^a/ \text{m}^2 \text{g}^{-1}$	$V_{\text{micro}}/ \text{cm}^3 \text{g}^{-1}$	$V_{\text{meso}}^b/ \text{cm}^3 \text{g}^{-1}$	$V_{\text{macro}}^b/ \text{cm}^3 \text{g}^{-1}$	$V_{\text{total}}/ \text{cm}^3 \text{g}^{-1}$	Ref.
NanoH-ZSM-5	475	11	464	0.18	0.15	0.23	0.56	this work
H-ZSM-5	432	1	431	0.15	0.04	–	0.19	30

^a t-Plot method. ^b NLDFT method, macropores at the 50–80 nm range.

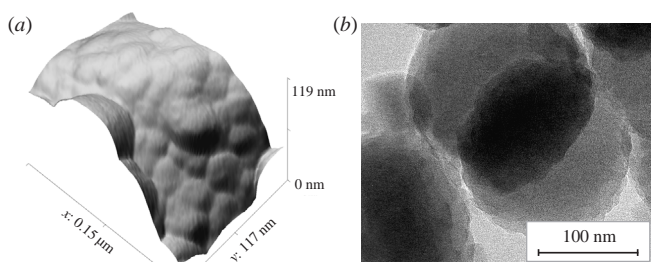


Figure 3 (a) AFM and (b) TEM images of aggregate of the synthesized nanoH-ZSM-5 zeolite.

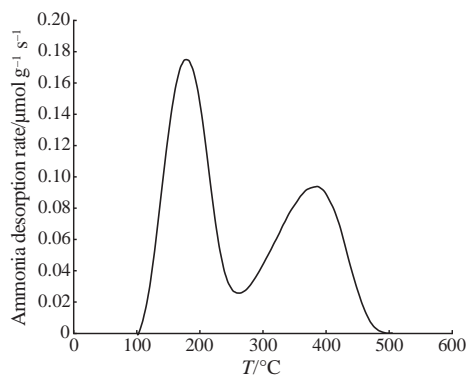


Figure 4 NH₃-TPD profile of nanoH-ZSM-5 zeolite.

Table 2 Acidic properties of nanoH-ZSM-5 and H-ZSM-5 zeolites.

Catalyst	Weak and medium strength ^a	Strong ^b	Total	Ref.
NanoH-ZSM-5	105	90	195	this work
H-ZSM-5	113	107	220	31

^a Calculated as amount of NH₃ (μmol g⁻¹) desorbed below 300 °C. ^b Calculated as amount of NH₃ (μmol g⁻¹) desorbed above 300 °C.

acidity of both zeolites are comparable. Meanwhile, weak and medium acid sites are dominating in nanoH-ZSM-5 zeolite.

Thus, a novel method of hydrothermal-microwave synthesis of a nanosized ZSM-5 zeolite with a predominant particle size of 30–80 nm directly in the proton form has been developed.

The properties of the obtained material allow us to consider it a promising catalyst for a number of petrochemical processes.

This research was carried out within the state funding TIPS RAS and IGIC RAS Center for Collective Use of Scientific Equipment.

Online Supplementary Materials

Supplementary data associated with this article can be found in the online version at doi: 10.1016/j.mencom.2024.04.039.

References

1. R. Wang, C. Xia and B. Peng, *Catal. Today*, 2022, **405–406**, 111.
2. Z. Wan, G. K. Li, C. Wang, H. Yang and D. Zhang, *Appl. Catal., A*, 2018, **549**, 141.
3. S. Lee and M. Choi, *J. Catal.*, 2019, **375**, 183.
4. L. Dai, N. Zhou, Y. Lv, K. Cobb, P. Chen, Y. Wang, Y. Liu, R. Zou, H. Lei, B. A. Mohamed, R. Ruan and Y. Cheng, *Sci. Total Environ.*, 2022, **847**, 157658.
5. Z. Yan, D. Chen, L. Huang, J. Liu, H. Fu, Y. Xiao and S. Li, *Microporous Mesoporous Mater.*, 2022, **337**, 111926.

6. M. Gao, Z. Gong, X. Weng, W. Shang, Y. Chai, W. Dai and L. Li, *Chin. J. Catal.*, 2021, **42**, 1689.
7. S. Hajimirzaee, A. S. Mehr and E. Kianfar, *Polycyclic Aromat. Compd.*, 2022, **42**, 2334.
8. H. O. Mohamed, R. K. Parsapur, I. Hita, J. L. Cerrillo, A. Ramírez, K.-W. Huang, J. Gascon and P. Castaño, *Appl. Catal., B*, 2022, **316**, 121582.
9. A. J. Mallette, S. Seo and J. D. Rimer, *Nat. Synth.*, 2022, **1**, 521.
10. E. Koohsaryan and M. Anbia, *Chin. J. Catal.*, 2016, **37**, 447.
11. Y. Ni, A. Sun, X. Wu, G. Hai, J. Hu, T. Li and G. Li, *J. Colloid Interface Sci.*, 2011, **361**, 521.
12. J. Jung, C. Jo, F. M. Mota, J. Cho and R. Ryoo, *Appl. Catal., A*, 2015, **492**, 68.
13. Y. Ji, B. Shi, H. Yang and W. Yan, *Appl. Catal., A*, 2017, **533**, 90.
14. A. Parulkar, R. Joshi, N. Deshpande and N. A. Brunelli, *Appl. Catal., A*, 2018, **566**, 25.
15. R. Zhang, P. Zhao, L. Han, J. Wang and L. Zhao, *Microporous Mesoporous Mater.*, 2021, **312**, 110754.
16. S. N. Talapaneni, J. Grand, S. Thomas, H. A. Ahmad and S. Mintova, *Mater. Des.*, 2016, **99**, 574.
17. Z. Chen, Z. Li, Y. Zhang, D. Chevella, G. Li, Y. Chen and J. Yu, *Chem. Eng. J.*, 2020, **388**, 124322.
18. A. Palčić and E. Catizzone, *Curr. Opin. Green Sustainable Chem.*, 2021, **27**, 100393.
19. K. K. Ramasamy, H. Zhang, J. Sun and Y. Wang, *Catal. Today*, 2014, **238**, 103.
20. H. Konno, T. Tago, Y. Nakasaka, R. Ohnaka, J.-I. Nishimura and T. Masuda, *Microporous Mesoporous Mater.*, 2013, **175**, 25.
21. M. Firooz, M. Baghalha and M. Asadi, *Catal. Commun.*, 2009, **10**, 1582.
22. H. Chen, Y. Wang, C. Sun, F. Gao, L. Sun, C. Wang, Z. Wang and X. Wang, *Catal. Commun.*, 2017, **100**, 107.
23. X. Mi, Z. Hou and X. Li, *Microporous Mesoporous Mater.*, 2021, **323**, 111224.
24. J. Shao, T. Fu, Q. Ma, Z. Ma, C. Zhang and Z. Li, *Microporous Mesoporous Mater.*, 2019, **273**, 122.
25. T. Xue, Y. M. Wang and M.-Y. He, *Microporous Mesoporous Mater.*, 2012, **156**, 29.
26. T. Fu, J. Chang, J. Shao and Z. Li, *J. Energy Chem.*, 2017, **26**, 139.
27. X. Zeng, X. Hu, H. Song, G. Hia, Z.-Y. Shen, R. Yu and M. Moskovits, *Microporous Mesoporous Mater.*, 2021, **323**, 111262.
28. Y. Hu, C. Li, Y. Zhang, N. Ren and Y. Tang, *Microporous Mesoporous Mater.*, 2009, **119**, 306.
29. A. G. Dedov, A. A. Karavaev, A. S. Loktev and P. V. Zemlianskii, *Patent RU 2787374*, 2023.
30. A. G. Dedov, A. A. Karavaev, A. S. Loktev, A. S. Mitinenko and I. I. Moiseev, *Catal. Today*, 2021, **367**, 199.
31. A. G. Dedov, A. A. Karavaev, A. S. Loktev, P. V. Zemlianskii, M. N. Vagapova, K. I. Maslakov, K. A. Cherednichenko, S. V. Egazar'yants, A. V. Khoroshilov and P. I. Ivanov, *Mendeleev Commun.*, 2023, **33**, 832.

Received: 6th December 2023; Com. 23/7334